REPORT DOCUMENTATION

AFRL-SR-BL-TR-99-

0208

1. AGENCY USE ONLY *(Leave blank)*	2. REPORT DATE	3. REPORT TYPE AND DATES COVERED
	1 November 1998	Final Technical Report 1 Apr 97 to 31 Dec 98

4. TITLE AND SUBTITLE
Instrumentation for Full Field Deformation Measurement with Nano-Second Resolution

5. FUNDING NUMBERS
F49620-97-1-0280

6. AUTHOR(S)
Horacio D. Espinosa

7. PERFORMING ORGANIZATION NAME(S) AND ADDRESS(ES)
School of Aeronautics and Astronautics
Purdue University
West Lafayette, IN 47906

8. PERFORMING ORGANIZATION REPORT NUMBER

9. SPONSORING/MONITORING AGENCY NAME(S) AND ADDRESS(ES)
Air Force Office of Scientific Research
Mathematics and Space Sciences
801 N. Randolph Street, Rm 732
Arlington, VA 22203-1977

10. SPONSORING/MONITORING AGENCY REPORT NUMBER
F49620-97-1-0280

11. SUPPLEMENTARY NOTES

12a. DISTRIBUTION AVAILABILITY STATEMENT
Approved for public release; distribution unlimited.

12b. DISTRIBUTION CODE

13. ABSTRACT *(Maximum 200 words)*
The Final Inventory of property which consists o:f Grantee Purchased Equipment, Ultra-High Speed CCd Camera and Components.

19990903 005

14. SUBJECT TERMS
Equipment

15. NUMBER OF PAGES
7

16. PRICE CODE

17. SECURITY CLASSIFICATION OF REPORT	18. SECURITY CLASSIFICATION OF THIS PAGE	19. SECURITY CLASSIFICATION OF ABSTRACT	20. LIMITATION OF ABSTRACT
Unclassified	Unclassfied	Unclassified	UL

INSTRUMENTATION FOR FULL FIELD DEFORMATION MEASUREMENT WITH NANO-SECOND RESOLUTION

Horacio D. Espinosa
School of Aeronautics and Astronautics
Purdue University
West Lafayette, IN 47906

AFOSR Award # F49620-97-1-0280

Final Technical Report

1. INTRODUCTION

The accurate evaluation of the dynamic fracture toughness of advanced materials is becoming increasingly important. Under dynamic fracture, material at the crack tip is strained suddenly, and if is rate sensitive, may offer more resistance to fracture than at quasi-static strain rates. High stain rate fracture testing is of interest because many structural components are subject to high loading rates in service or must survive high loading rates during accident conditions. Thus, these components must be designed against crack initiation under high loading rates or to arrest a rapidly propagating crack. The fracture toughness of a material loaded suddenly is generally higher than when the load is applied quasi-statically; therefore, dynamic toughness is an effective design parameters.

While there exists standardized method for determining the fracture toughness parameters K_{IC} and J_{IC} under quasi-static loading, to date, a unified view on the best measurement procedure to determine the dynamic fracture toughness of advanced materials has not been achieved. Hence, researchers still need to identify a simple and reliable experimental method capable of providing accurate dynamic fracture toughness measurements. Further understanding of the failure phenomena (such as crack propagation, material instabilities, etc.) in advanced layered and nano-materials require the development of novel experimental techniques. The motivation of the present investigation is to establish a reliable experimental/computational procedure to obtain both accurate dynamic fracture toughness and crack dynamic propagation parameters.

We are investigating failure modes by means of the impact of pre-cracked 4-point bending specimens. Two full field surface displacement measurements, dynamic white-light-speckle and coherent gradient sensing, are being used to examine strain fields at crack-tips in ceramics and layered-materials. A light gas gun and a Kolsky bar are employed to dynamically load the samples. Real time photographs are recorded using the Cordin Model 220 high-speed, 8-CCD, camera purchased under this grant. In combination with the measurement of dynamic load history, crack propagation using a crack gage, the following fracture parameters can be obtained from these full field tip images: 1) dynamic fracture toughness at initiation, 2) crack propagation speed and 3) stress intensity factor history.

2. RESEARCH METHODOLOGY

A stored-energy Kolsky bar as shown Figure 1 is employed to establish and calibrate the dynamic fracture measurement technique. Figure 2 shows the Single-Edge Notched Beam (SENB) samples used. During the test process, the SENB samples are mounted in the Kolsky bar and pre-loaded to keep them on position. The 5 Watt Verdi laser (Coherent Co.) is used to illuminate the sample using an optical beam splitter and a light diffuser. A Model K2 Infinity Long-Distance Microscope and the newly purchased high speed 8-CCD Cordin Camera model 220 (as shown in Figure 3), with up to 100 million frames per second, images the crack tip during sample deformation and failure. The high speed camera is triggered by a Tektronix model TDS520C oscilloscope with a frequency response up to 500MHz and a maximum sampling rate of 1Gs/s. The incident and transmitted loads are measured by two high frequency response load cells. The load cells are Quartz Load Washer Type 9001 from Kistler Co. with a range of 35KN. The load cells are used with a pre-load of 10% the maximum load to ensure stability and rapid response. A Charge Amplifier Model 5010B from Kistler Co. with a cut off frequency of 180 KHz is also utilized to energize the load cells. The crack initiation time is measure by a crack gauge that is glued on the sample. A schematic of the experimental setup is shown in Figure 4.

For the full field measurements, two full field measurement techniques are now being used, Speckle-Direct Image Correlation and coherent gradient sensing (CGS) techniques. When the crack tip display little plastic deformation, the Speckle-DIC method is ideal. By contrast, when large plasticity develops at the crack tip, CGS is used.

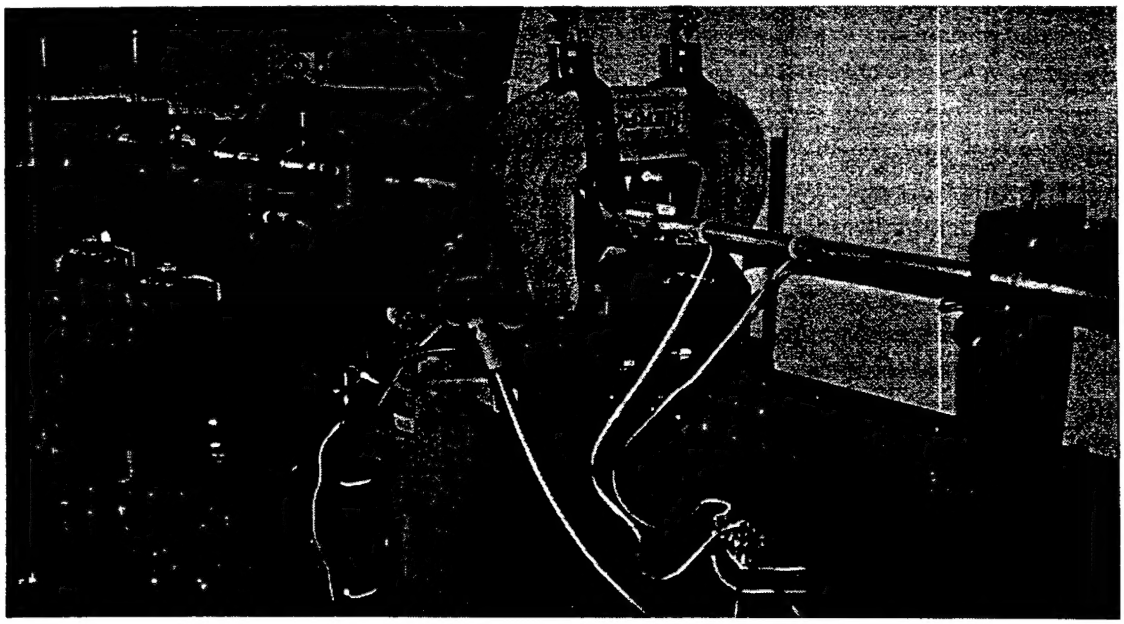

Figure 1: Picture of the stored-torque torsional Kolsky Bar Apparatus

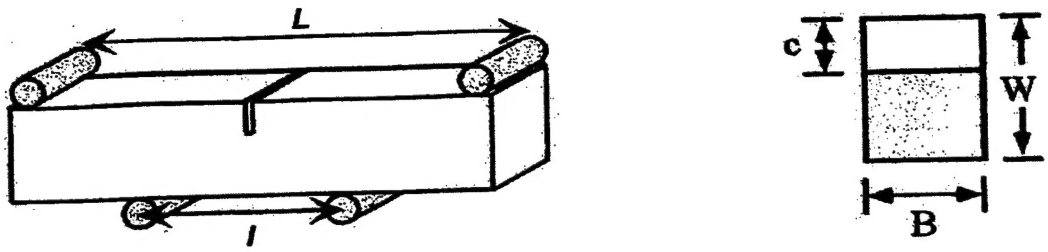

Figure 2: Single-Edge Notched Beam (SENB)

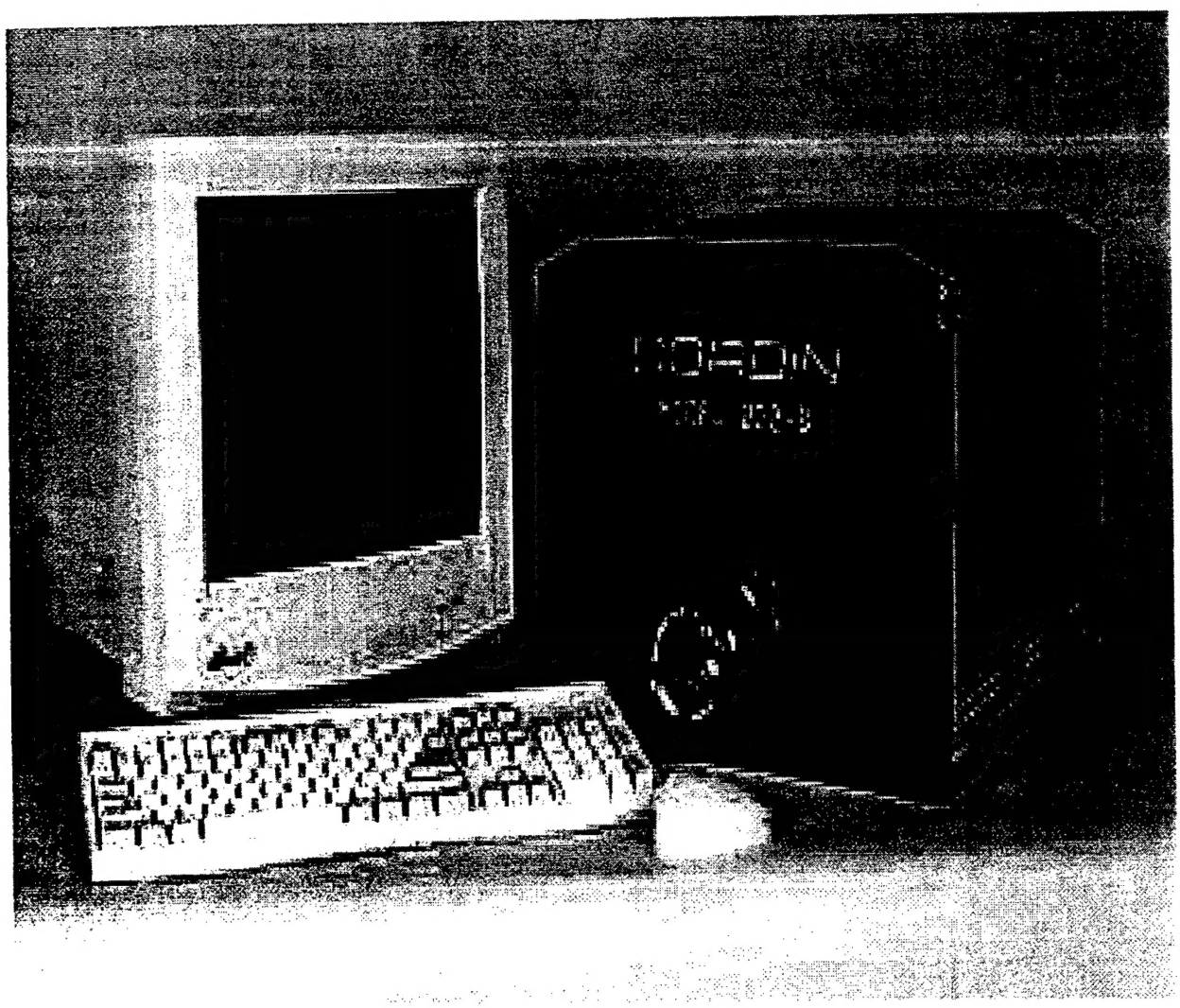

Figure 3: Cordin Model 220 high-speed 8-CCD camera

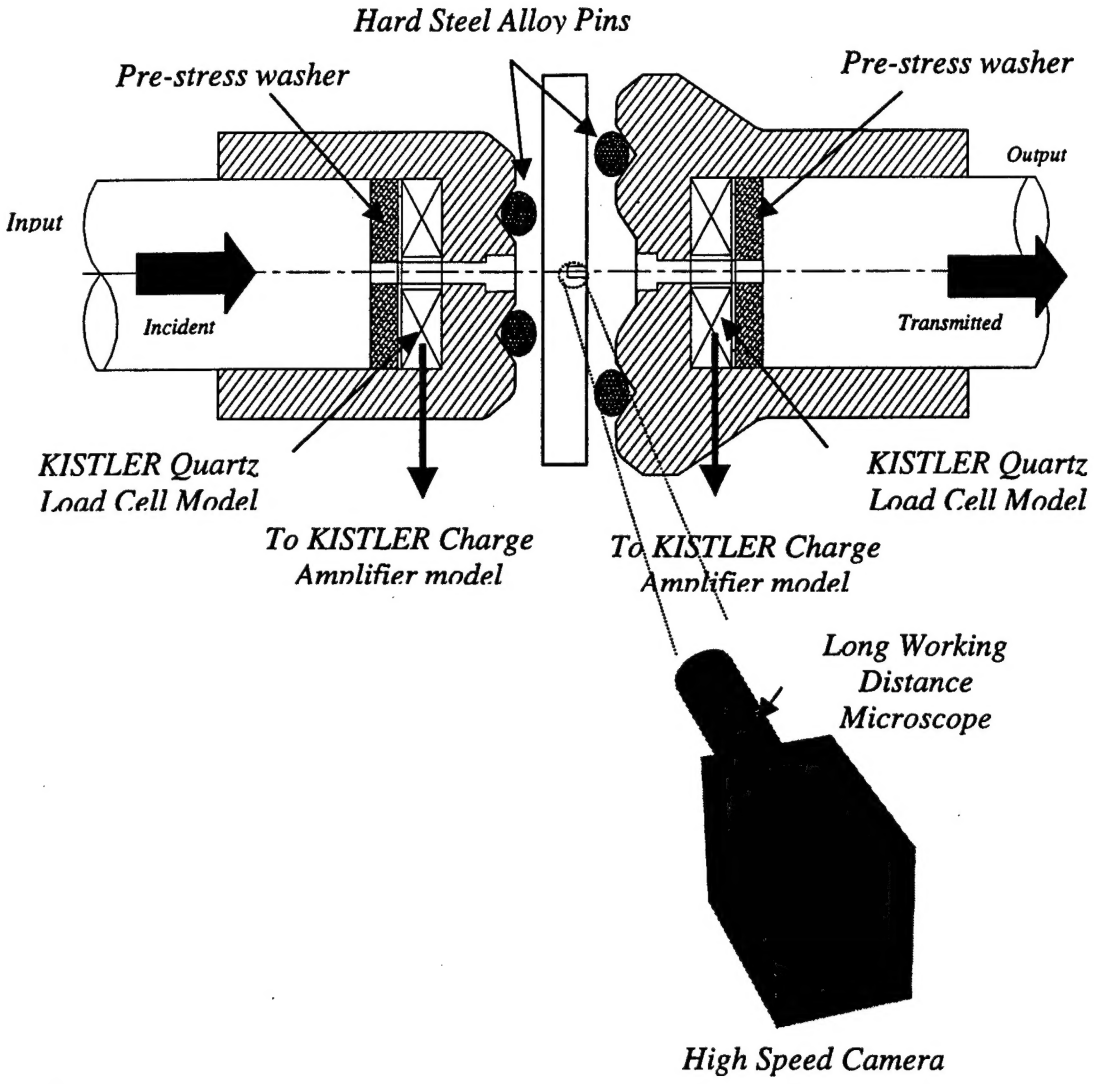

Figure 4: Schematic description of the experiment setup

2.1 Speckle-DIC Method

Figure 5 shows the detail Speckle-DIC setup in our Dynamic Inelasticity Laboratory. Before the test, the sample is mirror-polished. A random black-and-white speckle pattern is then produced on one surface of the sample and the crack gage is glued on the opposite surface.

Several tests were performed. Figure 6 shows the typical speckle images of SENB Aluminum specimens obtained using the present setup. The digitized images are currently being analyzed with digital correlation procedures to obtain the displacement and strain fields. With this full field information, in combination with crack initiation time, measured by the crack gage, and FEM simulations, the dynamic fracture toughness and stress intensity factor history of interest during the whole fracture process, will be obtained. We expect to correlate several experimental measurements in order to constrain the numerical simulations that are used to estimate K_{ID} or J_{ID}. In the case of brittle materials, the crack tip position history can be clearly seen in the images. From the tip positions, the average crack propagation speed can be estimated by dividing the relative distance of two near crack tip by the time difference.

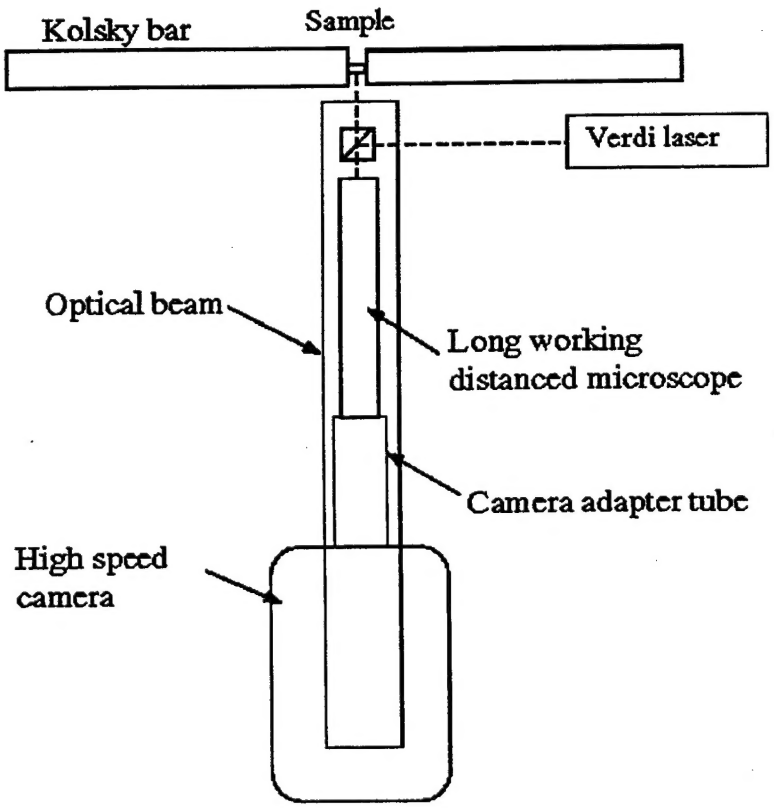

Figure 5: Speckle set-up

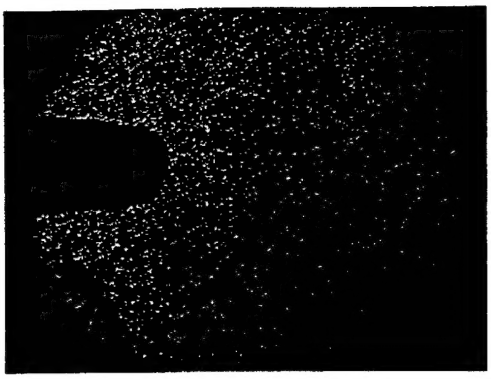

Picture 1: reference field

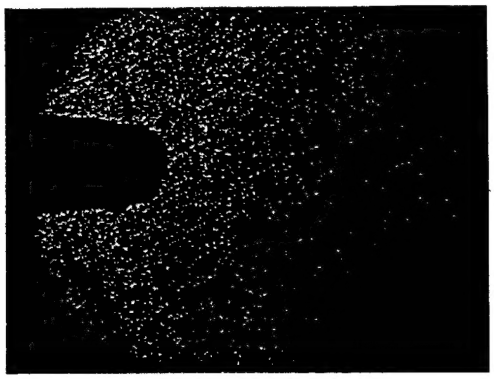

Picture 2: 20ms

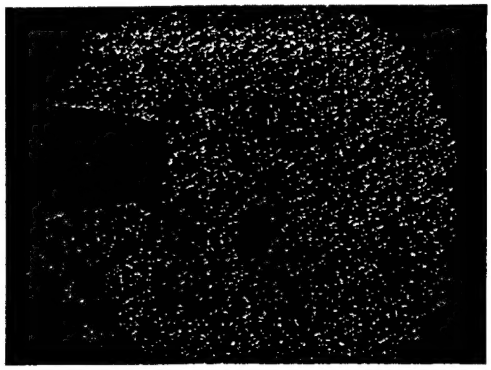

Picture 3: 100ms

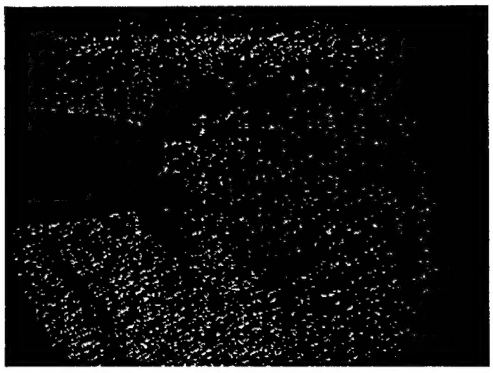

Picture 4: 200ms

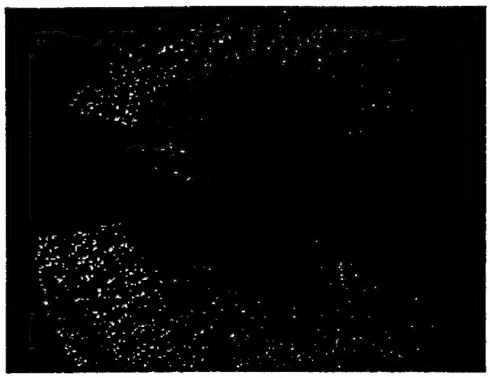

Picture 3: 300ms

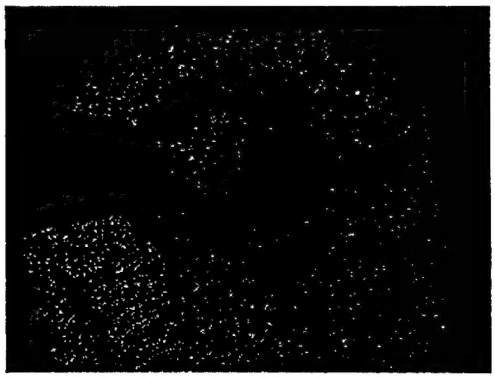

Picture 4: 500ms

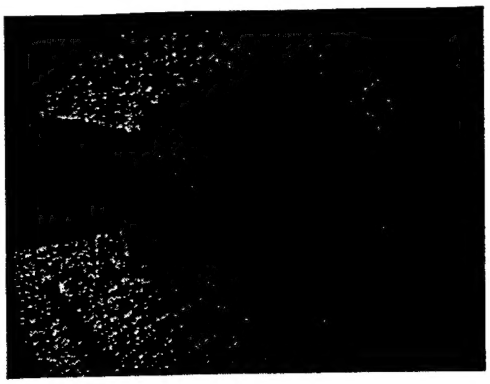

Picture 5: 700ms

Picture 6: 900ms

Figure 6: Speckle images of SENB Aluminum 6061-T6 Specimen

2.2 Coherent Gradient Sensing Method (CGS)

For some materials, large amounts of plasticity develop near the crack tip. CGS is the suitable full field measurement method in this case. Figure 7 shows the schematic setup of our present CGS test. The 5 Watt Verdi laser (Coherent Co.), optical components, specimen, and the Cordin Model 220 high speed camera are aligned precisely. The laser light must be perfectly perpendicular to the sample to obtain a working axis over which the optical setup is mounted. All CGS optical components are layed on that optical path. The sample surface is mirror-polished to achieve the desired reflectivity. The crack gage is glued on the back surface of the sample to provide a redundant measurement of crack speed.

Several tests were performed. Figure 8 shows typical high speed images of SENB PMMA specimens during the dynamic crack propagation process. From the images recorded with the high speed camera, we are now obtaining in-plane gradients of out-of-plane surface displacements around the crack tip. Since it is relatively insensitive to vibrations and rigid body motions, this technique has potential for dynamic crack growth measurements in advanced materials.

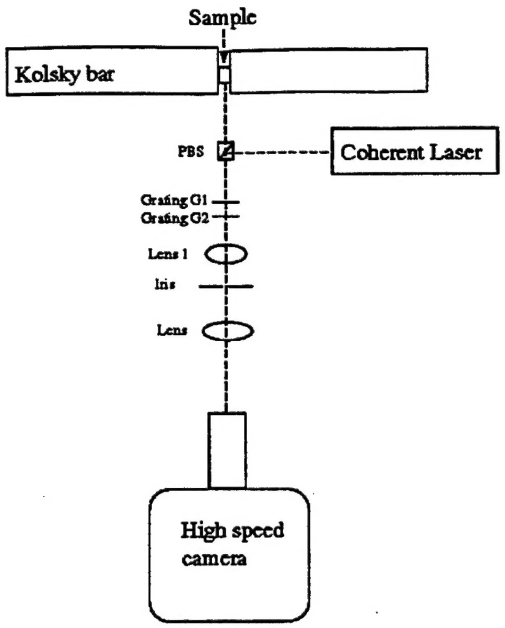

Figure 7: Schematic CGS Setup

Picture 1: 20ms

Picture 2: 100ms

Picture 3: 200ms

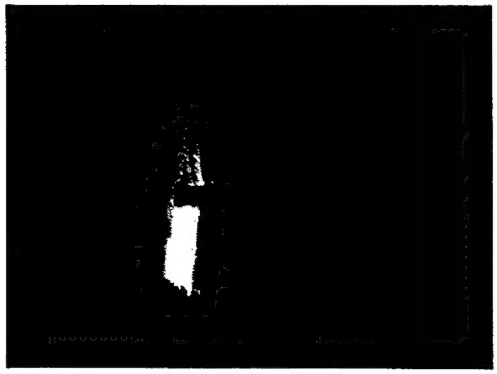

Picture 4: 300ms

Figure 8: High Speed Camera Images of PMMA SENB Specimen

3. DATA ANALYSIS

When a SENB sample is rapidly loaded, there are three typical time domains: short, intermediate, and long. In the short time domain, there is a complex wave propagation in the specimen and inertia effects dominates the specimen response. In this short time, reflecting stress waves that pass through the specimen constructively and destructively interfere with one another, resulting in a highly complex time-dependent stress distribution. It is not clear whether or not K or J-dominated field exists at this stage. In the intermediate time domain, the global inertia effects are significant but local oscillations at the crack are small. In the long time domain, the deformation dominates the specimen and K or J-dominated fields should exist. Nakamura et al. (1986) defined a *transition time*, t_τ, when the kinetic energy and the deformation energy are equal. Inertia effects dominate prior to the transition time, but the deformation energy dominates at time significantly greater than t_τ. In the latter case, a K or J-dominated field should exist near the crack tip and quasi-static relationships can be used to infer K or J from global load and displacement measurements. However, during the transition time, quasi-static relationships can not be used if crack propagation occurs before t_τ. The wave propagation phenomenon is a function of the material ductility. Brittle and fiber composite materials may not achieve a K or J-dominated condition. Hence, in-depth investigations are required to gain insight into these features.

Based on elastic Bernoulli-Euler beam theory, Nakamura et al.(1986) proposed a formula for the transition time, viz.,

$$t_\tau = D\Lambda\frac{W}{C_o}$$

Where D is a displacement coefficient defined by

$$D = \frac{t\dot{\Delta}(t)}{\Delta(t)},$$

Λ is a geometry factor , W is the specimen width, C_0 is the longitudinal wave speed of the materials, Δ is the loading line displacement, and $\dot{\Delta}(t)$ is the displacement rate. For the 3-point bending specimen, Λ is given by

$$\Lambda = \sqrt{\frac{SEBC}{W}}.$$

If fracture occurs after 2 t_τ, then it is normally thought that the static formulas for fracture toughness can provide an accurate quantification of J_{IC} or K_{IC}.

It is worth mentioning that for ductile materials, the transition time requirement can be met by decreasing the displacement rate or the width of the specimen, but for brittle materials, this requirement is difficult to meet. It is obvious that the static formula can not be used if the dynamic fracture properties of running cracks and the effect of high loading rated on fracture are of interest. In those circumstances, a dynamic data interpretation method should be used to de-convolute experimental test data. In the experimental process, there are

significant differences between ductile and brittle materials. So we will discuss them separately.

3.1 Ductile materials

For ductile materials, it has been suggested that, provided a one parameter representation of the crack tip fields remains valid, dynamic fracture toughness J_D can be a condition for onset of crack growth. If the plasticity near the crack tip is small, the K_D can be an alternative of J_D. To date relatively little experimental work has been done on determining fracture parameters for ductile fracture under dynamic loading conditions. Although some attempts have been made, the data interpretation is still based on quasi-static formulae for J. Simple and reliable test methods for characterizing dynamic fracture toughness in metals has not been established.

Theoretically, the transition time requirement can be met by decreasing the displacement rate or the width of the specimen. It is obvious that this requirement can not be met if the dynamic fracture properties of fast propagating cracks or high loading rates are of interest. In such cases, dynamic data interpretation methods should be used. In this situation, the dynamic fracture toughness J_D can be estimated by relating it to the measured crack tip opening displacement (CTOD) history. The details of the analysis procedure are the following:

a.) Asymptotic elastic-plastic crack tip field

Hutchinson (1968) and Rice and Rosengren (1968), collectively referred to as HRR, considered the case of monotonically loaded stationary crack in a material described by a J_2-deformation theory of plasticity and a power law hardening relationship between the plastic strain and stress. They showed that the strain components in the crack tip region scale with the value of the J-integral. Within a small strain assumption, the asymptotic solution of the elastic-plastic field equations, in the crack tip region, has the form

$$\varepsilon_{ij} \rightarrow \varepsilon_o \left[\frac{J}{\sigma_o \varepsilon_o I_n r} \right]^{n/(n+1)} E_{ij}(n,\sigma)$$

$$\sigma_{ij} \rightarrow \sigma_o \left[\frac{J}{\sigma_o \varepsilon_o I_n r} \right]^{n/(n+1)} \Sigma_{ij}(n,\sigma)$$

as $r \rightarrow 0$. σ_o is the tensile yield stress, ε_o is the equivalent tensile yield strain, n is the hardening exponent. The dimensionless quantity, I_n, is defined by Hutchinson (1968). The amplitude factor J is the value of Rice's J-integral (Rice, 1968). It has been suggested that, provided a one parameter representation of the crack tip fields remains valid, a condition for onset of crack growth is the attainment of a critical value of J.

b.) Crack tip opening displacement (CTOD) associated with the HRR singular field

If the CTOD is defined using the intersection of a 90^o vertex with the crack flanks as shown in Figure 9 (Shih, 1981), the J-integral can be related to CTOD using the HRR singularity field as

$$J = \frac{\sigma_o}{d_n(\varepsilon_o, n)}\delta$$

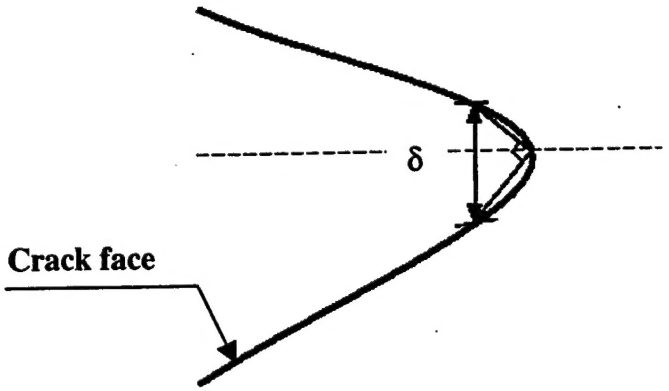

Figure 9: CTOD defined by Shih (1981)

where , δ is the CTOD, J is the value of J-integral, σ_o is the yield stress and d_n is a material dependent dimensionless constant as defined by Shih. (1981). For dynamic loading, the above equation becomes

$$J(t) = \frac{\sigma_o}{d_n(\varepsilon_o, n)}\delta(t).$$

At crack initiation time, $J_D = J(t_i)$, in which t_i is defined as the crack propagation time.

The CTOD can be obtained either experimentally or numerically.

The first method is to obtain the CTOD at crack initiation time directly from high speed camera images. Typical speckle pictures are shown in Figure 5. If at the crack initiation time the CTOD is measured, the J_D can be obtained directly from the above formula.

Another method to identify CTOD is using FEM simulations with the incident loading and transmitted loading, recorded with load cells, as input loading conditions. The CTOD defined above can be obtained from the FEM solutions and therefore the J_D can then be obtained with the numerically CTOD at the crack initiation time measured experimentally. Alternatively, a calculation of J can be performed and $J_D = J(t_i)$ computed.

3.2 Brittle materials:

For brittle materials, it is very difficult to meet the transition time requirement. Hence, the dynamic data analysis should be performed in almost all the time domain. Plasticity is supposed to be very small close to the crack tip and a dynamic stress intensity factor K is supposed to control the crack behavior. In the present study, the dynamic

fracture toughness K_D will be estimated by correlating the displacement from experiment with those from asymptotic solution.

a.) Asymptotic elastic-plastic crack tip field

The asymptotic crack tip field under steady-state conditions is given as an infinite series by Nishioka et al.(1983). The displacement fields under Mode I condition can be written as

$$U=\sum_{n=1}^{\infty}\frac{K_n B_I(C)}{2\mu}\sqrt{\frac{\pi}{2}}(n+1)\left\{r_1^{\frac{n}{2}}\cos(\frac{n\theta_1}{2})-h(n)r_2^{\frac{n}{2}}\cos(\frac{n\theta_2}{2})\right\}$$

$$V=\sum_{n=1}^{\infty}\frac{K_n B_I(C)}{2\mu}\sqrt{\frac{\pi}{2}}(n+1)\left\{-\beta_1 r_1^{\frac{n}{2}}\sin(\frac{n\theta_1}{2})-\frac{1}{\beta_2}h(n)r_2^{\frac{n}{2}}\sin(\frac{n\theta_2}{2})\right\}$$

where

$$C_l=\sqrt{\frac{(\kappa+1)\mu}{(\kappa-1)\rho}} \qquad C_t=\sqrt{\frac{\mu}{\rho}}$$

$$\beta_1=\sqrt{1-\left(\frac{C}{C_l}\right)^2} \qquad \beta_2=\sqrt{1-\left(\frac{C}{C_t}\right)^2}$$

$$\theta_m=\tan^{-1}\frac{\beta_m y}{x} \qquad r_m=\sqrt{x^2+\beta_m^2 y^2} \quad \text{m=1,2}$$

$$h(n)=\frac{2\beta_1\beta_2}{1+\beta_2^2} \text{ for odd n} \qquad h(n)=\frac{1+\beta_2^2}{2} \text{ for even n}$$

$$B_I(C)=\frac{1+\beta_2^2}{D} \qquad D=4\beta_1\beta_2-(1+\beta_2^2)^2$$

C is the speed of the propagating crack tip, $\kappa=(3-\nu)/(1+\nu)$ for the plane stress conditions, ν is Possion's ratio, μ is the shear modulus of elasticity and ρ is the density. In the series solution, the coefficient of the first term K_1 is equal to K(t). At the crack initiation time, $K_D=K(t_i)$.

A region on the specimen in which the most singular term of the asymptotic expansion, for the above displacements, describes the actual displacement field is called a K-dominant region. If experimental displacement data are taken at point (x, y) exhibiting such a K-dominant region then extraction of K_D can be obtained by performing a least-squares fitting procedure of the above equation. FEM simulation can be employed to decide the near crack tip three-dimensional region. When analyzing the experimental displacement data, data points lying within this region, are excluded since this is a three-dimensional deformation zone.

Although the above asymptotic field has the steady-state assumptions (i.e., constant crack tip speed), the assumption is acceptable in deciding the dynamic fracture initiation toughness.

b.) Determination of displacement fields experimentally

In order to use the above solutions to identify the dynamic fracture toughness, displacement fields must be measured. At present, two methods will be used: speckle-DIC and FEM simulation.

In the speckle method, a subset, such as 10X10 mm^2, near the crack tip will be chosen and will be correlated digitally from one image to another. Once the location of this subset in the deformed images is found, displacement of this subset is known. The dynamic fracture toughness is obtained through comparing the DIC displacement with asymptotic displacement field. The fracture toughness is then obtained at the crack initiation time.

In the FEM simulation method, the incident load and the transmitted load obtained from the experiment are used as the FEM input load conditions. FEM simulations are then used to obtain the displacement field. The Dynamic fracture toughness is obtained through comparison of the FEM displacement with measured displacement field at initiation time. The fracture toughness is then obtained at the crack initiation time.

The present methodology also allows the study of running cracks at constant speed (steady state) or even through FEM simulations the K_D quantification for the case of accelerating cracks.

4. FUTURE WORK

The present method will be further developed so that it can be employed to study dynamic failure mechanisms of nano-materials and layered materials under various dynamic loading conditions and various environmental conditions (high and low temperatures). The effect of material microstructure on the dynamic failure of advanced materials will be studied using the methodology previously discussed.

New techniques that can trace the development and propagation of material instabilities in advanced materials will also be developed combining high speed photography, laser and optical techniques. This will help the understanding of mechanisms leading to shear band initiation, propagation and related failure phenomena. With these investigations, shear band initiation and propagation criterion of advanced materials will be established.

5. PERSONNEL

Principal Investigator: H.D. Espinosa

Graduate Students: H. V. Arrieta, A. Patanella, H. Zhang

6. REFERENCES

1. Nakamura, T., C.F. Shih and L.B. Freud (1986) Analysis of a dynamically loaded three-point-bending ductile fracture specimen. *Engineering Fracture Mechanics* **25**, 323-339.
2. Bohme, W. and Kalthoff , J.F. (1982) The behabior of notched bend specimens in impact testing, *International journal of fracture* **20**, R139-R143.
3. Kalthoff, J. F. (1985) On the measurement of dynamic fracture toughness- a review of recent work. *International journal of fracture* **27**, 277-298.
4. Yokoyama, T. and Kishida, K. (1989) A novel impact three-point bend test method for determining dynamic fracture-initiation toughness", *Experimental Mechanics*, **June**, 188-194.
5. Duffy, J., Suresh, S. Cho, K. and Bopp, E. R. (1988) A method for dynamic fracture initiation testing of ceramics. *Journal of Material technology* **110**, 325-331.
6. Kathoff, J. F. (1986) Fracture behavior under high rates of loading. *Engineering Fracture Mechanics* **23**, 289-298.
7. Chevallier, J. M., Ansart, J. P. and Dormeval, R.(1984), Fracture toughness of some metals under high loading rate conditions. *Proc. Third Conf. Mechanical Properties of Materials at high strain rates of strain. Institute of physics, Conference Series* No.**70**, 229-236.
8. Nakano, M. and Kishida, K. (1990) Measurement of dynamic fracture toughness by longitudinal impact of pre-cracked round bar. *International journal of pressure & piping* **44**, 3-15.
9. Hutchinson, J. W. (1968) Singular behavior at the end of a tensile crack in a hardening material. *Journal of the Mechanics and Physics of Solids* **16** , 13-31.
10. Rice, J. R. (1968) and Rosengren, G. F. (1968) Plane strain deformation near a crack tip in a power-law-hardening material. *Journal of the Mechanics and Physics of Solids* **16**, 13-31.
11. Rice, J. R. (1968) A path independent integral and the approximate analysis of a strain concentration by notches and cracks. *Journal of Applied Mechanics* **35**, 379-386.
12. Shih, C. F. (1981) Relationships between the J-integral and the crack tip opening displacement for stationary and extending cracks. *Journal of the Mechanics and Physics of Solids* **29**, 305-326.
13. Nishioka, T. and Atluri, S. N. (1983) Path-independent integrals, energy release rate, and general solution of sear-tip fields in mixed-mode dynamic fracture. *Engineering Fracture Mechanics* **18**, 1-22.
14. Krishnaswamy, S., Rosakis, A. J. and Ravichandran, G (1991) On the extent of dominance of asymptotic elastodynamic crack-tip fields: II. Numerical investigation of three-dimensional and transient effects. *Journal of Applied Mechanics* **58**, 95-103.
15. Rosakis, A. J. and Ravi-Chandar, K. (1986) On crack-tip stress states: An experimental evaluation of three dimensional effects. *International journal of solid structure* **22**, 121-134.